Radio Science, Volume 33, Number 4, Pages 919–928, July–August 1998

Water vapor microwave continuum absorption: A comparison of measurements and models

Philip W. Rosenkranz
Research Laboratory of Electronics, Massachusetts Institute of Technology, Cambridge

Abstract. Measurements, made in different laboratories, of absorption by water vapor in microwave windows are compared with models for the water vapor continuum. A reanalysis of some of these measurements leads to the conclusion that the laboratory data are best represented by a combination of *Liebe*'s [1987] millimeter-wave propagation model (MPM) for the foreign-broadened component of the water continuum and the 1993 version of MPM for the self-broadened component. This combined model is validated by comparison with measurements of atmospheric microwave emission.

1. Introduction

Since the pioneering measurements of *Becker and Autler* [1946], it has been known that the absorption of microwaves by water vapor is not entirely attributable to nearby spectral lines. Models for atmospheric water vapor transmittance therefore include an empirical component which is called the "continuum," in addition to line contributions. This practice is also followed in infrared transmittance models. Strictly speaking, the distinction between local-line and continuum absorption is arbitrary, because only the total absorption can be measured. The continuum is what remains after subtraction of line contributions, and the latter depend on the number of lines considered, on their intensities, and on their shapes, which may or may not have a cutoff. However, using reasonable definitions, it can be said that the water vapor continuum contributes most of the opacity of a clear midlatitude or tropical atmosphere at window frequencies of 30 GHz or higher.

Other laboratory measurements of water vapor's microwave-window absorption have been made by *Frenkel and Woods* [1966], *Liebe* [1984], *Liebe and Layton* [1987], *Godon et al.* [1992], and *Bauer et al.* [1993, 1995, 1996]. There is a consensus that the continuum has two components: one proportional to the square of water vapor partial pressure, the other proportional to the product of water vapor and foreign-gas partial pressures. The first component has a much stronger dependence on temperature than the second. These characteristics indicate that the second component is due to binary interactions involving a water molecule and a foreign-gas molecule, while the first component originates in interactions between two water molecules, at distances close enough that the deep potential well formed by these polar molecules is important. However, one cannot distinguish between bound-state and free interactions (collisions) on the basis of the temperature dependence.

Ma and Tipping [1990] give a theoretical treatment of continuum absorption by pure water vapor, in which the absorption is due to the collision-broadened far wings of the numerous submillimeter and far-infrared resonances. Another theory, "third-order linear absorption," in which pairs of water molecules cooperatively absorb photons while both molecules undergo transitions in internal energy, has been put forward by *Hudis et al.* [1991, 1992]. Other authors have speculated about collision-induced absorption and dimer absorption bands. Without intending to prejudge the issue of their origin, the two components of the continuum described above will be denoted by the terms "self-broadened continuum" and "foreign-broadened continuum" in this paper.

The continuum problem is still open to theoretical investigations, but it appears that at present, atmospheric calculations rely on empirical models for the continuum. Within the past decade, a large body of experimental work has been produced by the groups led by H. Liebe

Paper number 98RS01182.
0048-6604/98/98RS-01182$11.00

and A. Bauer. The present paper reviews these results and empirical models based on them and suggests a resolution of some of the discrepancies, which leads to a recommended model for atmospheric radiative transfer calculations.

2. Local-Line Contribution to Absorption

Local-line absorption is calculated here as

$$\alpha_{\text{line}} = n\sum_i S_i(T)\left[f_i(\nu)+f_i(-\nu)\right], \tag{1}$$

in which n is the number density of water molecules, ν is frequency, and the line intensities $S(T)$, which are functions of temperature T, are calculated from the HITRAN database [*Rothman et al.*, 1992]. The 15 lines listed in Table 1 are included in the summation. The line shape $f_i(\nu)$ incorporates a cutoff at ν_c = 750 GHz and subtracted baseline, as given by *Clough et al.* [1989]:

$$f_i(\nu)=\begin{cases}\left(\nu^2\gamma_i/\pi\nu_i^2\right)\left\{\left[(\nu-\nu_i)^2+\gamma_i^2\right]^{-1}-\left[\nu_c^2+\gamma_i^2\right]^{-1}\right\}, & |\nu-\nu_i|<\nu_c,\\ 0, & |\nu-\nu_i|\ge\nu_c,\end{cases} \tag{2}$$

where ν_i is the line center frequency and γ_i is the line half width, which is calculated as

$$\gamma = w_s P_{H_2O}\theta^{x_s} + w_f P_f \theta^{x_f}, \tag{3}$$

where w_s, x_s, w_f, and x_f are constant coefficients; θ = 300/T, with T in kelvins; P_{H_2O} is the partial pressure of water vapor; and P_f is the partial pressure of dry air components. For reference, the width coefficients are also listed in Table 1. They differ only in minor respects from the values used by *Liebe* [1989]. In his model, Liebe included an additional 15 lines, which are negligible for the data to be considered here, being either weaker or lying outside the range $|\nu-\nu_i|<\nu_c$.

If $\nu_c \to \infty$, (1) and (2) combined would be equivalent to a Van Vleck-Weisskopf line shape. The imposition of a cutoff at 750 GHz has some practical advantages. The Van Vleck-Weisskopf line shape, and others such as Gross and Lorentz, are based on the approximation of instantaneous collisions (the impact approximation), which restricts their validity to frequencies not very distant from resonance. The cutoff avoids applying the line shape to distant frequencies and also establishes a limit to the summation in (1). *Clough et al.*'s [1989] choice of 750 GHz is to some degree arbitrary, but it is followed here.

Table 1. Line Parameters

Frequency, GHz	w_f, GHz/kPa	x_f	w_s, GHz/kPa	x_s
22.2351	0.0281	0.69	0.1349	0.61
183.3101	0.0281	0.64	0.1491	0.85
321.2256	0.0230	0.67	0.1080	0.54
325.1529	0.0278	0.68	0.1350	0.74
380.1974	0.0287	0.54	0.1541	0.89
439.1508	0.0210	0.63	0.0900	0.52
443.0183	0.0186	0.60	0.0788	0.50
448.0011	0.0263	0.66	0.1275	0.67
470.8889	0.0215	0.66	0.0983	0.65
474.6891	0.0236	0.65	0.1095	0.64
488.4911	0.0260	0.69	0.1313	0.72
556.9360	0.0321	0.69	0.1320	1.00
620.7008	0.0244	0.71	0.1140	0.68
752.0332	0.0306	0.68	0.1253	0.84
916.1716	0.0267	0.70	0.1275	0.78

Data are from *Liebe and Dillon* [1969], *Liebe et al.* [1969], and *Bauer et al.* [1987, 1989].

One might pose the question, Why not consider models using other line shapes? In particular, the Gross line shape has greater absorption in its low-frequency wing than does the Van Vleck-Weisskopf. However, the need for an empirical continuum, although a smaller one, still exists with the Gross line shape, so this constitutes a weak argument for it. If the continuum is used to repair deficiencies in the far line wings, then it would seem most sensible to choose the line shape that best represents absorption in the vicinity of resonances. *Hill* [1986] compared the Van Vleck-Weisskopf, Gross, and full Lorentz line shapes with *Becker and Autler*'s [1946] measurements near 22 GHz and found that the verdict of the data was definitively in favor of Van Vleck-Weisskopf. This conclusion does not necessarily apply to other lines, but as the ratio of width to center frequency decreases, these three line shapes become close to one another near resonance.

3. Pure Water Vapor

As mentioned above, the continuum absorption arising from water self-broadening is proportional to the

square of pressure (or density). It is also well known that the frequency dependence of the microwave spectrum of any molecule is that of the Fourier-transformed autocorrelation function of the dipole moment responsible for the absorption, multiplied by the square of frequency [see, e.g., *Clough et al.*, 1989; *Ma and Tipping*, 1990]. Hence a reduced continuum absorption is defined here as

$$C_s = \nu^{-2}\theta^{-3}P_{H_2O}^{-2}(\alpha - \alpha_{line}), \quad (4)$$

where α is the total measured absorption in pure water vapor. The product θP_{H2O} is proportional to gas density, and the third factor of θ in (4) is introduced due to stimulated emission; C_s will be examined for residual variation with temperature and frequency, using measurements.

Figure 1 plots measurements of C_s, as defined by (4), from H. Liebe's and A. Bauer's laboratories at frequencies ranging from 138 to 239 GHz. In this case of self-broadening, the correction for α_{line} ranges from 3 to 15% of the actual measurements at these frequencies. Although there are differences at any given temperature

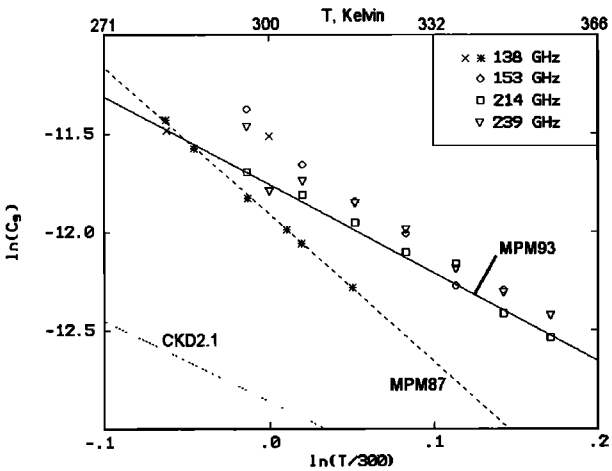

Figure 1. Self-broadened continuum coefficient (equation (4)), measured in pure water vapor: crosses indicate data from *Liebe* [1984]; asterisks indicate data from *Liebe and Layton* [1987]; circles indicate data from *Bauer et al.* [1993]; squares indicate data from *Godon et al.* [1992]; and triangles indicate data from *Bauer et al.* [1995]. Model calculations are from *Liebe and Layton* [1987](MPM87); *Liebe et al.* [1993](MPM93); and *Clough et al.* [1989](CKD2.1). The units of C_s are (dB/km)/(GHz kPa)^2.

of up to 60% between the highest and lowest values of C_s, there is no consistent trend with frequency; in fact, often the highest measurements are those at 153 GHz (circles) while the lowest are at 138 GHz (asterisks).

Ma and Tipping [1990] raised the issue of whether the frequency and temperature dependences of the continuum can be factored into product form, as is commonly done in empirical models. In their calculations, the inverse temperature dependence of C_s steepens as frequency increases. Any such trend is not evident in Figure 1; for example, the 239-GHz data (triangles) are intermediate between those at 153 GHz (circles) and 214 GHz (squares) in slope. Of course, the possibility that a variation in slope might become manifest over a wider range of frequency cannot be excluded.

Also represented in Figure 1 are continuum models MPM87, which is based on the *Liebe and Layton* [1987] measurements (also described by *Liebe* [1989]); MPM93, derived by *Liebe et al.* [1993] from various measurements including his own and those of *Godon et al.* [1992]; and the zero-wavenumber limit of CKD2.1 [*Clough et al.*, 1989], which is a model for the infrared as well as the microwave continuum. It appears that microwave data may not have been given sufficient weight in the derivation of the CKD model, which is too low in C_s.

Considering the absence of consistent variations with frequency in either magnitude or slope of $\ln(C_s)$ versus $\ln(T/300)$, it appears probable that the differences between measurements at any given temperature in Figure 1 are due to systematic errors. These measurements involve numerous difficulties, such as absorption of vapor on cavity walls and the low values of absorption at window frequencies. MPM93 provides a reasonable compromise fit to the entire ensemble of measurements in Figure 1, even though the measurements at 153 and 239 GHz were not available at that time. MPM93 was formulated in terms of a "pseudo-line"; however, at frequencies below 800 GHz it can be represented simply as

$$C_s = 7.8\times10^{6}\theta^{4.5}, \quad (5)$$

in units of (dB/km)/(GHz×kPa); θ=300/T is dimensionless. Equation (5) includes a minor (+3%) adjustment to compensate for the use of equation (2) instead of a Van Vleck-Weisskopf line shape, but this is not a substantive alteration of the model. (The same adjustment was also applied to MPM87 in Figure 1.)

4. Water Vapor Mixed With Other Gases

When binary interactions apply, absorption due to water vapor in air can be modeled by

$$\alpha = \alpha_{line} + \nu^2\theta^3\left(C_f P_f P_{H_2O} + C_s P_{H_2O}^2\right), \quad (6)$$

where C_f is a coefficient that may depend on temperature and frequency. The measurements under consideration here are all at frequencies such that $(\nu - \nu_i)^2 >> \gamma_i^2$; hence the partial-pressure dependence of α_{line} is due to the products $n\gamma_i$. Thus, at each particular frequency and temperature, α_{line} can be represented by a sum of two terms similar to the continuum (but with different coefficients). Then the partial-pressure dependence of total measured absorption can be expressed as

$$\alpha = a P_f P_{H_2O} + b P_{H_2O}^2 + c P_f^2, \quad (7)$$

where a, b, and c are coefficients that depend on frequency and temperature. The last term on the right side of (7) is contributed by collision-induced absorption in nitrogen, by oxygen, etc.; it is typically 2 orders of magnitude smaller than the other terms in the laboratory measurements discussed here, and when the foreign-gas partial pressure is constant, it may be lumped together with cavity losses.

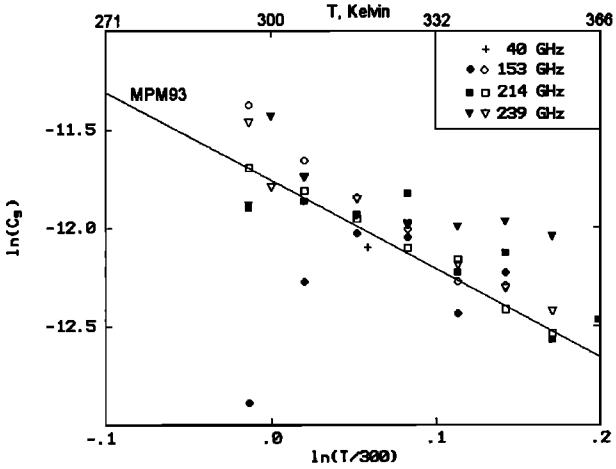

Figure 2. Comparison of self-broadened continuum coefficient measured in pure water vapor (symbols are the same as in Figure 1) with the self-broadened component of the continuum measured in an H_2O-N_2 mixture (solid symbols, same references) or in moist air (plus sign) [*Becker and Autler*, 1946].

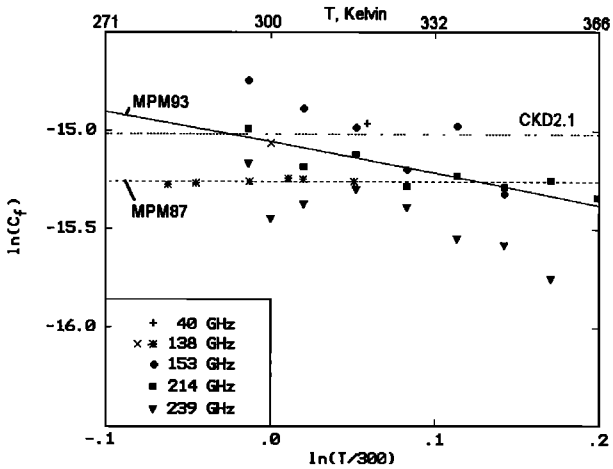

Figure 3. Measurements of the foreign-broadened component of the water vapor continuum; symbols are the same as in Figures 1 and 2. The measurements in moist nitrogen (cross and solid symbols) have been reduced by 12% for comparison with the moist-air measurements (plus sign and asterisks).

Experimental procedures on mixtures have differed: *Liebe and Layton* [1987] first introduced pure water vapor into the cavity and measured its absorption at pressures up to a few kilopascals. Dry air was then added; measurements were taken at several pressures up to approximately one atmosphere, with the water content fixed. *Godon et al.* [1992] and *Bauer et al.* [1993, 1995] measured H_2O-N_2 mixtures with a fixed N_2 partial pressure of 750 torr (100 kPa) but varying H_2O partial pressures. *Becker and Autler* [1946] held total pressure at one atmosphere while varying the water content of moist air. They made their measurements at a single temperature of 318 K.

Godon et al. [1992] and *Bauer et al.* [1993, 1995] fitted quadratic curves to their H_2O-N_2 data independently of the pure H_2O data. Figure 2 compares the C_s from Figure 1 with the values of C_s obtained by subtracting the local-line contribution from their b coefficients. Also plotted is a C_s obtained from *Becker and Autler*'s [1946] 40-GHz moist-air data. Figure 2 shows that although the two ways of measuring C_s yield roughly comparable values, the scatter of data points obtained from the H_2O-N_2 mixtures is greater than for pure H_2O.

Figure 3 plots C_f values resulting from subtraction of α_{line} from measured a coefficients. Here α_{line} accounts for 20-30% of a. For a, it is also necessary to take into account the greater broadening effectiveness of H_2O-N_2

collisions than of H_2O-O_2 collisions. For H_2O-N_2 data, a has been reduced by 12% for comparison with air mixtures. This ratio was measured by *Liebe and Layton* [1987] at 303 K and 138 GHz, and it is assumed to apply at other temperatures and frequencies. *Bauer et al.* [1989] measured nearly the same ratio (1.09) for w_f at 183 GHz.

In Figure 3 there is a larger variation than in Figure 1 among points at any given temperature; but here also, one cannot identify a consistent trend with frequency. The highest values tend to be found at 153 GHz, and the lowest tend to be found at either 138 GHz or 239 GHz. The 40-GHz and 214-GHz measurements are intermediate. Also shown in Figure 3 are curves computed from the MPM87, MPM93, and CKD2.1 models. As in the case of the self-broadened continuum, MPM87 was derived from the data of *Liebe and Layton* [1987] alone, whereas MPM93 appears as a compromise fit between that data and other measurements, especially *Godon et al.* [1992].

Another interpretation of the data of *Godon et al.* [1992] and *Bauer et al.* [1993, 1995] is possible because they measured self-broadening separately in pure water vapor and in moist nitrogen. They fitted quadratic curves to the moist nitrogen data by itself. One could instead fix the b coefficient at the value b' obtained from pure water vapor and fit the moist nitrogen data with

$$\alpha - b' P_{H_2O}^2 = a' P_f P_{H_2O} + c' P_f^2, \tag{8}$$

with a' and c' adjustable. This is similar to the way that *Liebe* [1984] and *Liebe and Layton* [1987] interpreted their data. The least squares solutions of (7) and (8) are related (see the appendix). For the case of an unskewed distribution of P_{H_2O}, which applies here,

$$a' = a + 2(b - b')\langle P_{H_2O} \rangle / P_f, \tag{9}$$

where $\langle P_{H_2O} \rangle$ is the mean value of P_{H_2O}; in the measurements of *Godon et al.* [1992] and *Bauer et al.* [1993, 1995], $\langle P_{H_2O} \rangle$ was approximately 2.13 kPa and P_f was fixed at 100 kPa.

Figure 4 shows an example of the two methods of fitting a curve to some of the data of *Bauer et al.* [1993]; they plotted the solid curve as a quadratic regression in the form of (7), and the dashed curve is obtained from (9). To evaluate (9), b' was obtained from Table 1 of *Bauer et al.* [1993], which represents a power law function of temperature fitted to their pure water vapor

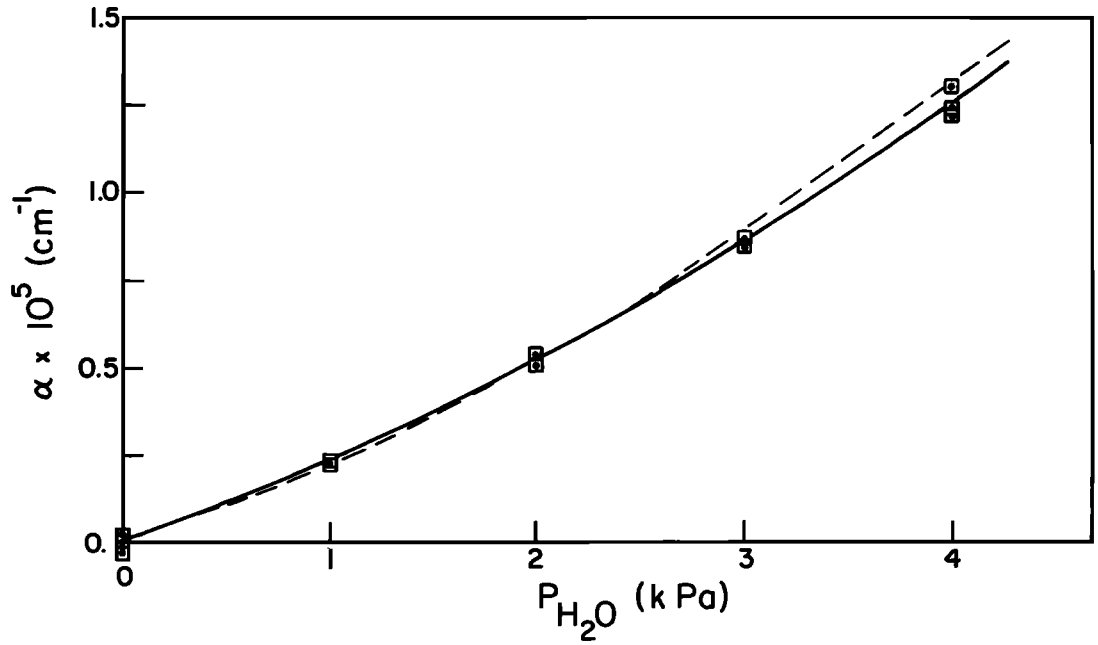

Figure 4. Absorption at 153 GHz and 316 K, in a mixture of 100-kPa N_2 and water vapor at partial pressure P_{H_2O}, from *Bauer et al.* [1993]. Solid curve indicates free quadratic fit to data; dashed curve indicates quadratic constrained to be consistent with pure water vapor absorption at the same frequency.

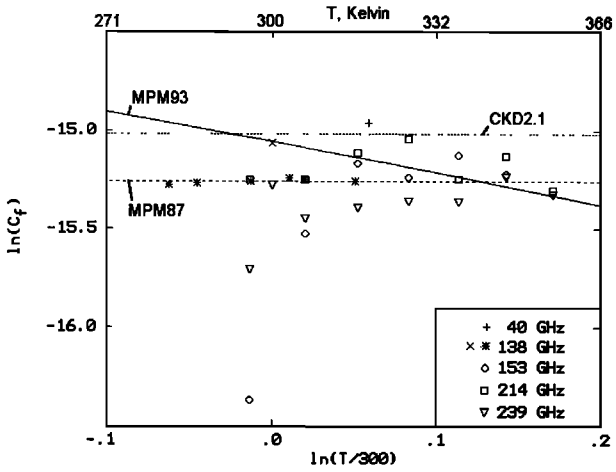

Figure 5. Measurements of the foreign-broadened continuum component, as in Figure 3, except that the data plotted by open symbols have been readjusted to be consistent with pure water vapor absorption at the same frequencies.

data; this should reduce random errors. Of course, the solid curve fits the data with lower residuals because it has one more free coefficient. However, when more coefficients are extracted by regression, each coefficient becomes less certain as an individual value. Considering the scatter of the data points, the dashed line does not do violence to the data. An argument in favor of it is that, as seen in Figure 2, the pure water vapor measurements yield values of C_s with less scatter than obtained from H_2O-N_2 mixtures.

Figure 5 shows the measurements of Figure 3, with the *Godon et al.* [1992] and *Bauer et al.* [1993, 1995] data adjusted using (9). (The single data point from *Becker and Autler* [1946] was not readjusted because they made no pure water vapor measurements.) Except for two outliers at 296 K, this readjustment reduces the spread of the measurements. Furthermore, it appears from this figure that revision of the MPM87 model for the foreign-broadened continuum, as in MPM93, is not justified. For use with the cutoff line shape in equation (2), the MPM87 model for C_f in air is

$$C_f = 2.36\times10^{-7}(dB/km)(GHz\times kPa)^{-2}. \qquad (10)$$

It has been increased by 15% over the original value [*Liebe*, 1987, 1989] which was intended for use with a Van Vleck-Weisskopf line shape without cutoff.

5. Atmospheric Absorption and Emission

On the basis of the discussion in sections 3 and 4, the best model for the water vapor continuum should be a combination of the foreign-broadened continuum from MPM87 and the self-broadened continuum from MPM93. As a shorthand notation, this combination will be called MPMf87/s93 here. In the atmosphere, the higher values of water vapor mixing ratio, for which self-broadening is significant, are found in the temperature range of approximately 270-300 K. From Figure 1, it can be seen that MPM93 and MPM87 differ only slightly in this range, with respect to the self-broadened continuum. Consequently, the predictions of MPMf87/s93 will be close to those of MPM87 in atmospheric applications. Hence the good agreement of MPM87 calculations with field measurements at 90, 96, and 330-430 GHz found by *Westwater et al.* [1990], *Manabe et al.* [1989], and *Liebe* [1987], respectively, is not contradicted.

In Figures 6-8, zenith brightness temperatures computed using equation (6) and the continuum models discussed above are compared with atmospheric microwave emission at 90 GHz, measured by *Westwater*

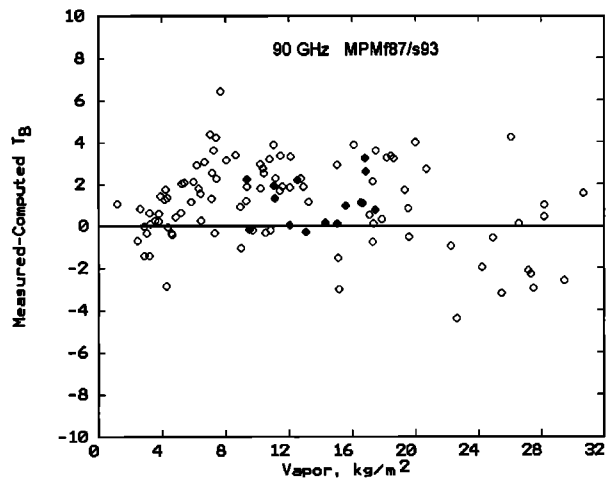

Figure 6. Differences between measured zenith brightness temperatures from *Westwater et al.* [1990] and calculations, using the MPM87 foreign-broadened water continuum plus the MPM93 self-broadened water continuum. Open symbols indicate data from Denver, Colorado; solid symbols indicate data from San Nicolas Island, California.

et al. [1990]. Differences are plotted versus the precipitable water content of the contemporaneous radiosonde profile. Absorption due to oxygen and nitrogen in the atmosphere was computed using the models of *Liebe et al.* [1992] and *Rosenkranz* [1993], respectively, for all cases here. At 90 GHz the dry components of the atmosphere contribute ~10 K to the zenith brightness temperature, while water vapor contributes up to ~60 K in these calculations. In Figure 6, MPMf87/s93 yields a scatter diagram with a bias of the order of 2 K but without any clear dependence on the water vapor content. A constant bias could result from an error in the oxygen model, which is fitted to measurements made in the frequency range of 49-67 GHz and therefore constitutes an extrapolation at 90 GHz. A scatter diagram (not shown) using the MPM87 model for both components of the water continuum was nearly indistinguishable from Figure 6.

It is illuminating to compare Figure 7, where the CKD2.1 model was used, and Figure 8, in which MPM93 was used, with Figure 6. The foreign-broadened continuum in CKD2.1 is ~30% higher than in MPM87, while the self-broadened continuum of CKD2.1 is roughly 3 times smaller than in MPM93. These differences tend to cancel in an atmosphere with a moderate amount of water vapor. Thus, even though the components of the continuum models are very different, it would be difficult to choose between CKD2.1 and MPMf87/s93 solely on the basis of the data in Figures 6 and 7. In Figure 8, on the other hand, the discrepancies with observations are evident, even though in a certain sense the MPM93 model is closer to that of Figure 6, because it differs only in the foreign-broadened component. From these examples, we must conclude that although measurements of atmospheric emission can be sensitive to absorption model errors, they are not necessarily well suited for extraction of separate components of the model.

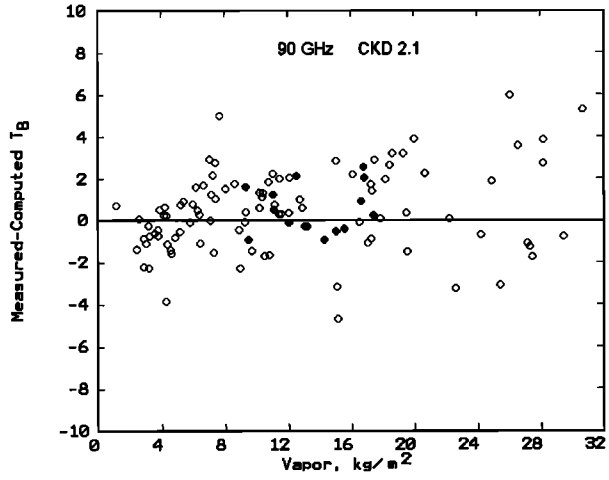

Figure 7. Same as in Figure 6, except calculations use the CKD2.1 continuum.

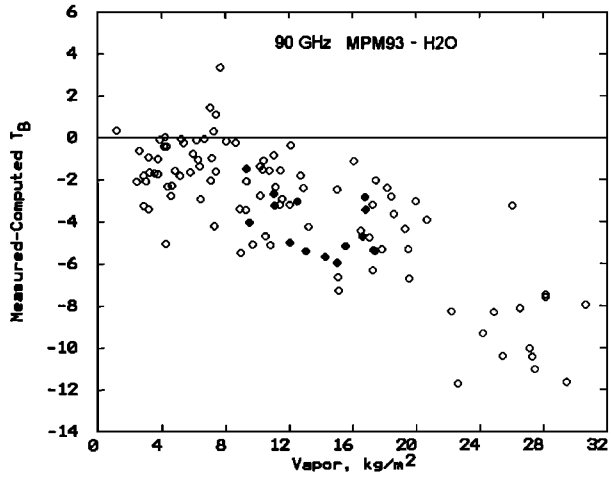

Figure 8. Same as in Figure 6, except calculations use MPM93 for both components of the water continuum.

Scatterplots for *Westwater et al.*'s [1990] 31.65-GHz data (not shown) lead to the same conclusions as Figures 6-8, although this frequency is less sensitive to continuum absorption than 90 GHz. It should be noted that the comparisons in Figures 6-8 depend on the accuracy of radiosonde calibration [*Clough and Brown*, 1995].

In Figures 9 and 10, up-looking brightness temperatures at 89 and 157 GHz, respectively, measured from an aircraft by *English et al.* [1994], are compared with calculations using the three water continuum models. Data from three flights in different climates are plotted in each figure. The atmospheric temperature and moisture profiles were measured up to 9 km by the aircraft's instrumentation, and above that altitude they were measured by radiosondes. H990 was a cold and dry atmosphere with 15 kg/m^2 vapor, A012 was a warm and less dry (23 kg/m^2 vapor) atmosphere, and A143 was a tropical atmosphere with 45 kg/m^2 water vapor. Figures 9 and 10 show similar results at both frequencies. In the

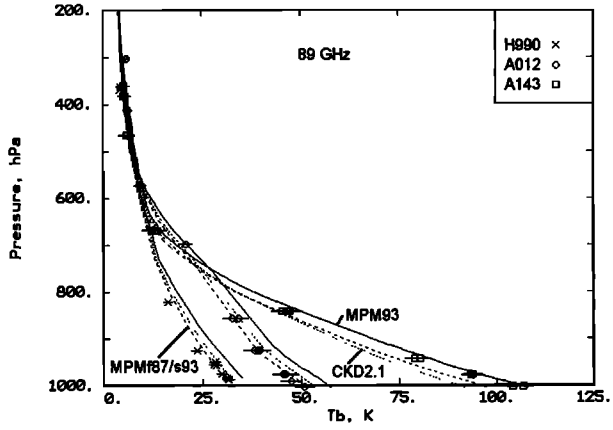

Figure 9. Near-zenith 89-GHz brightness temperatures measured by *English et al.* [1994], and calculations using three water vapor continuum models. The short horizontal lines through the data points are error brackets. H990 data are from northern Finland; A012 data are from the eastern Mediterranean; and A143 data are from near Ascension Island.

first two flights, MPMf87/s93 (dashed lines) yields the closest overall fit to the measurements, MPM93 (solid lines) predicts substantially higher brightness temperatures at most altitudes, and the CKD2.1 model (dotted lines) is intermediate. In A143, however, the measurements at lower altitudes are nearly as high as MPM93. MPMf87/s93 does not predict enough absorption in A143, while CKD2.1 is even lower. Calculations using MPM87 for both continuum components, given by *English et al.* [1994], are very close to the MPMf87/s93 brightness temperatures for all three flights.

English et al. [1994] suggest that an increase in the self-broadened component of the MPM water continuum would yield better agreement with their measurements. The MPM self-broadened continuum contributes 35 K to the 157-GHz brightness temperature at the surface in A143. Corresponding values for H990 and A012 are 5 K and 14 K, respectively. Hence an increase in the self-broadened component could help to move MPMf87/s93 closer to the data from A143, but preservation of good agreement in the other two atmospheres would require a simultaneous downward adjustment of the foreign-broadened component. These adjustments would be of a magnitude that would be hard to reconcile with the laboratory measurements and the ground-based radiometer data discussed above.

At pressure levels less than ~500 hPa, the absorption at 89 GHz is mostly due to oxygen. However, the excess of measurement over calculation which appeared in Figure 6 does not have a counterpart in Figure 9 at the lower pressures.

6. Summary and Conclusions

In this paper, several adjustments were made to published laboratory measurements and models, which are as follows:

1. The foreign-broadening coefficients obtained by *Bauer et al.* [1993, 1995] and *Godon et al.* [1992] were adjusted by using the self-broadening coefficients measured by the same experimenters in pure H_2O.
2. Measurements of foreign broadening by nitrogen were adjusted to be comparable to air.
3. Absorption due to 15 local lines was subtracted from the measurements, using a cutoff version of the Van Vleck-Weisskopf line shape.
4. The amplitudes of the MPM continuum components were adjusted to be compatible with the use of a cutoff line shape, i.e., when compared with the data from which the original models were derived.

After these adjustments, the combination of foreign-broadened water continuum from *Liebe and Layton* [1987] and self-broadened continuum from *Liebe et al.* [1993] appears to provide the most satisfactory overall representation of currently available data. However, there will always be errors in both laboratory and atmospheric measurements, so no continuum model will be perfect. There are some issues that require further study, such as very moist atmospheres and the question of possible variation of the temperature dependence with frequency.

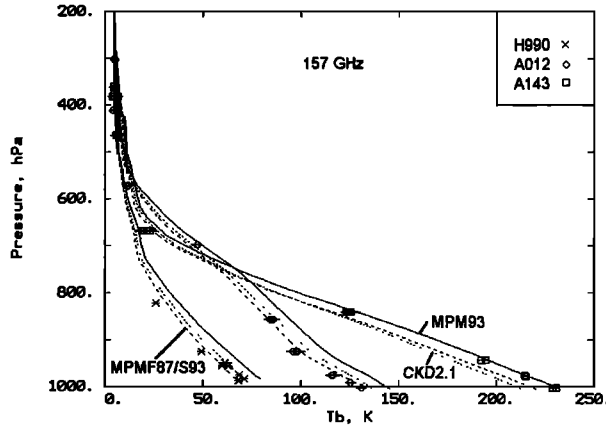

Figure 10. Same as in Figure 9, except at 157 GHz.

Theoretical calculations can make a major contribution to understanding the water vapor continuum. To put these calculations on a footing as sound as that of line broadening near resonance, they should make use of accurate intermolecular potentials such as those of *Franken and Dykstra* [1994a, b]. The useful comparisons that could be made between theory and measurements include temperature and frequency dependence of both self and foreign components and variation of the latter component with different perturber molecules.

Appendix: Quadratic Regression Equations

Given an ensemble of values for two variables x and y, the quadratic function

$$\hat{y}(x) = \sum_{i=0}^{2} c_i x^i \tag{A1}$$

that minimizes $\left\langle \{y - \hat{y}(x)\}^2 \right\rangle$, where the angle brackets denote an average over the ensemble, can be determined from

$$c_0 = \langle y \rangle - c_1 \langle x \rangle - c_2 \langle x^2 \rangle \tag{A2}$$

and

$$[c_1, c_2]^T = \langle YX^T \rangle \langle XX^T \rangle^{-1}, \tag{A3}$$

where $Y = y - \langle y \rangle$ and the elements of the vector $X = [X_1, X_2]^T$ are defined as

$$X_1 = x - \langle x \rangle \tag{A4}$$

and

$$X_2 = x^2 - \langle x^2 \rangle. \tag{A5}$$

Solution of (A3) yields

$$c_1 = \{\langle YX_1 \rangle \langle X_2^2 \rangle - \langle YX_2 \rangle \langle X_1 X_2 \rangle\} / D \tag{A6}$$

and

$$c_2 = \{\langle YX_2 \rangle \langle X_1^2 \rangle - \langle YX_1 \rangle \langle X_1 X_2 \rangle\} / D, \tag{A7}$$

in which

$$D = \langle X_1^2 \rangle \langle X_2^2 \rangle - \langle X_1 X_2 \rangle^2. \tag{A8}$$

Now let us assume that the second-order coefficient is known a priori to have the value c_2', and we wish to find c_0', c_1' in the function

$$\hat{y}'(x) = \sum_{i=0}^{2} c_i' x^i, \tag{A9}$$

such that $\left\langle \{y - \hat{y}'(x)\}^2 \right\rangle$ is minimized. The solution is

$$c_0' = \langle y \rangle - c_1' \langle x \rangle - c_2' \langle x^2 \rangle, \tag{A10}$$

$$c_1' = \{\langle YX_1 \rangle - c_2' \langle X_1 X_2 \rangle\} / \sigma_x^2, \tag{A11}$$

where $\sigma_x^2 = \langle X_1^2 \rangle$. To relate c_1' to c_1 and c_2, $\langle YX_2 \rangle$ is eliminated from (A6)-(A7), and the resulting equation is solved for $\langle YX_1 \rangle$, which when substituted in (A11) yields

$$c_1' = c_1 + (c_2 - c_2') \langle X_1 X_2 \rangle / \sigma_x^2. \tag{A12}$$

Using the definitions of X_1 and X_2, we have

$$\langle X_1 X_2 \rangle = \langle X_1^3 \rangle + 2 \langle x \rangle \sigma_x^2. \tag{A13}$$

Thus, in the case that $\langle X_1^3 \rangle = 0$, one obtains

$$c_1' = c_1 + 2(c_2 - c_2') \langle x \rangle, \tag{A14}$$

which is equivalent to equation (9) when $x = P_{H_2O}$, $y = \alpha$, $a = c_1 / P_f$, and $b = c_2$.

Acknowledgments. The author thanks S. English and E.R. Westwater for their data, S.A. Clough and A. Bauer for helpful conversations on water vapor absorption, and D.H. Staelin for comments on the manuscript. This work was begun while the author was a visiting scientist at the U.K. Meteorological Office and continued with support from M.I.T. Lincoln Laboratory.

References

Bauer, A., M. Godon, M. Kheddar, J.M. Hartmann, J. Bonamy, and D. Robert, Temperature and perturber dependences of water-vapor 380 GHz line broadening, *J. Quant. Spectrosc. Radiat. Transfer, 37*, 531-539, 1987.

Bauer, A., M. Godon, M. Kheddar, and J.M. Hartmann, Temperature and perturber dependences of water vapor line-broadening: Experiments at 183 GHz; calculations below 1000 GHz, *J. Quant. Spectrosc. Radiat. Transfer, 41*, 49-54, 1989.

Bauer, A., M. Godon, J. Carlier, Q. Ma, and R.H. Tipping, Absorption by H2O and H2O-N2 mixtures at 153 GHz, *J. Quant. Spectrosc. Radiat. Transfer, 50*, 463-475, 1993.

Bauer, A., M. Godon, J. Carlier, and Q. Ma., Water vapor absorption in the atmospheric window at 239 GHz, *J. Quant. Spectrosc. Radiat. Transfer, 53*, 411-423, 1995.

Bauer, A., M. Godon, J. Carlier, and R.R. Gamache, Absorption of a H2O-CO2 mixture in the atmospheric window at 239 GHz; H2O-CO2 linewidths and continuum, *J. Mol. Spectrosc. 176*, 45-57, 1996.

Becker, G.E., and S.H. Autler, Water vapor absorption of electromagnetic radiation in the centimeter wave-length range, *Phys. Rev., 70*(5/6), 300-307, 1946.

Clough, S.A., and P.D. Brown, Intercomparison of radiance algorithms for the microwave, in *Optical Remote Sensing of the Atmosphere*, OSA Tech. Dig. Ser., vol. 2, pp. 74-75, Opt. Soc. of Am., Washington, D. C., 1995.

Clough, S.A., F.X. Kneizys, and R.W. Davies, Line shape and the water vapor continuum, *Atmos. Res., 23*, 229-241, 1989.

English, S.J., C. Guillou, C. Prigent, and D.C. Jones, Aircraft measurements of water vapour continuum absorption at millimetre wavelengths, *Q. J. R. Meteorol. Soc., 120*, 603-625, 1994.

Franken, K.A., and C.E. Dykstra, A water-water potential derived using a quantum Monte Carlo vibrational analysis, *J. Chem. Phys., 100*(4), 2865-2870, 1994a.

Franken, K.A., and C.E. Dykstra, Quantum Monte Carlo vibrational analysis of the nitrogen-water complex, *Chem. Phys. Lett., 220*, 161-166, 1994b.

Frenkel, L., and D. Woods, The microwave absorption by H2O vapor and its mixtures with other gases between 100 and 300 Gc/s, *Proc. IEEE, 54*(4), 498-505, 1966.

Godon, M., J. Carlier, and A. Bauer, Laboratory studies of water vapor absorption in the atmospheric window at 213 GHz, *J. Quant. Spectrosc. Radiat. Transfer, 47*, 275-285, 1992.

Hill, R.J., Water vapor-absorption line shape comparison using the 22-GHz line: The Van Vleck-Weisskopf shape affirmed," *Radio Sci., 21*(3), 447-451, 1986.

Hudis, E., Y. Ben-Aryeh, and U.P. Oppenheim, Third-order linear absorption by pairs of molecules, *Phys. Rev. A, 43*(7), 3631-3639, 1991.

Hudis, E., Y. Ben-Aryeh, and U.P. Oppenheim, The contribution of third order linear absorption to the water vapor continuum, *J. Quant. Spectrosc. Radiat. Transfer, 47*, 319-323, 1992.

Liebe, H.J., The atmospheric water vapor continuum below 300 GHz, *Int. J. Infrared Millimeter Waves, 5*(2), 2c7-227, 1984.

Liebe, H.J., A Contribution to modeling atmospheric millimeter-wave properties, *Frequenz, 41*, 31-36, 1987.

Liebe, H.J., MPM-An atmospheric millimeter-wave propagation model, *Int. J. Infrared Millimeter Waves, 10*(6), 631-650, 1989.

Liebe, H.J. and T.A. Dillon, Accurate foreign-gas-broadening parameters of the 22-GHz H2O line from refraction spectroscopy, *J. Chem. Phys., 50*(2), 727-732, 1969.

Liebe, H.J., and D.H. Layton, *Millimeter-wave properties of the atmosphere: Laboratory studies and propagation modeling*, NTIA Rep. 87-224, Natl. Telecommun. and Inf. Admin., Boulder, Colo., 1987.

Liebe, H.J., M.C. Thompson Jr., and T. A. Dillon, Dispersion studies of the 22 GHz water vapor line Shape, *J. Quant. Spectrosc. Radiat. Transfer, 9*, 31-47, 1969.

Liebe, H.J., P.W. Rosenkranz, and G.A. Hufford, Atmospheric 60-GHz oxygen spectrum: New laboratory measurement and line parameters, *J. Quant. Spectrosc. Radiat. Transfer, 48*, 629-643, 1992.

Liebe, H.J., G.A. Hufford, and M.G. Cotton, Propagation modeling of moist air and suspended water/ice particles at frequencies below 1000 GHz, *AGARD Conf. Proc. 542*, 3.1-3.10, 1993.

Ma, Q., and R.H. Tipping, "Water vapor continuum in the millimeter spectral region, *J. Chem. Phys., 93*(9), 6127-6139, 1990.

Manabe, T., R.O. Debolt, and H.J. Liebe, Moist-air attenuation at 96 GHz over a 21-km line-of-sight path," *IEEE Trans. Antennas and Propag., 37*(2), 262-266, 1989.

Rosenkranz, P.W., Absorption of microwaves by atmospheric gases, in *Atmospheric Remote Sensing by Microwave Radiometry* , edited by M. A. Janssen, chap. 2, pp. 37-90, John Wiley, New York, 1993.

Rothman, L.S., et al., The Hitran molecular database: Editions of 1991 and 1992, *J. Quant. Spectrosc. Radiat. Transfer, 48*, 469-507, 1992.

Westwater, E.R., J.B. Snider, and M.J. Falls, Ground-based radiometric observations of atmospheric emission and attenuation at 20.6, 31.65, and 90.0 GHz: A comparison of measurements and theory, *IEEE Trans. Antennas and Propag., 38*(10), 1569-1580, 1990.

P.W. Rosenkranz, Massachusetts Institute of Technology Room 26-343, 77 Massachusetts Avenue, Cambridge, MA 02139. (e-mail: pwr@mit.edu)

(Received October 3, 1997; revised February 24, 1998; accepted April 9, 1998.)